

Rotation induced superfluid-normal phase separation in trapped Fermi gases

M. Iskin and E. Tiesinga

*Joint Quantum Institute, National Institute of Standards and Technology,
and University of Maryland, Gaithersburg, Maryland 20899-8423, USA.*

(Dated: February 3, 2022)

We use the Bogoliubov-de Gennes formalism to analyze the effects of rotation on the ground state phases of harmonically trapped Fermi gases, under the assumption that quantized vortices are not excited. We find that the rotation breaks Cooper pairs that are located near the trap edge, and that this leads to a phase separation between the nonrotating superfluid (fully paired) atoms located around the trap center and the rigidly rotating normal (nonpaired) atoms located towards the trap edge, with a coexistence (partially paired) region in between. Furthermore, we show that the superfluid phase that occurs in the coexistence region is characterized by a gapless excitation spectrum, and that it is distinct from the gapped phase that occurs near the trap center.

PACS numbers: 03.75.Hh, 03.75.Kk, 03.75.Ss

With the ultimate success of techniques for trapping and cooling atomic gases developed and improved gradually since the 1980s, atomic Fermi gases have emerged as unique testing grounds for many theories of exotic matter in nature, allowing for the creation of complex yet very accessible and controllable many-body quantum systems. For instance, evolution from the weakly attracting Bardeen-Cooper-Schrieffer (BCS) limit to the weakly repulsive molecular Bose-Einstein condensation (BEC) have been observed in a series of remarkable experiments. The ground state phases of such atomic Fermi gases have since been the subject of intense theoretical and experimental research worldwide [1, 2].

To verify the superfluid ground state of atomic Fermi gases, it is essential to analyze their response to rotation. For instance, it has been theoretically predicted that sufficiently fast rotation of superfluid Fermi gases excites quantized vortices in the form of hexagonal vortex lattices [3, 4, 5]. Such vortex lattices have recently been observed for both population balanced [6] and imbalanced [7] systems. These vortex experiments have not only complemented previously found signatures, but also provided the ultimate evidence to support the superfluid nature of the ground state.

Recently, the effects of rotation on the ground state phases of harmonically trapped Fermi gases has been theoretically studied at unitarity, under the assumption that quantized vortices are not excited [8] (see also Ref. [9]). It has been argued that the rotation causes a complete phase separation between a nonrotating superfluid core and a rigidly rotating normal gas, with a discontinuous density at the interface. Subsequently, this problem has been analyzed using the mean-field BCS framework within the semi-classical local density approximation (LDA) [10]. In addition to the superfluid and normal regions, a coexistence region is found, the possibility of which is not considered in Ref. [8].

In this manuscript, we go beyond the semi-classical LDA and develop a quantum mechanical Bogoliubov-de Gennes (BdG) formalism to analyze the effects of rotation on the ground state phases of harmonically trapped Fermi gases. We discuss both population balanced and imbalanced mixtures throughout the BCS-BEC evolution. Our main results are in qualitative agreement with those of Ref. [10]. We find that the rotation breaks Cooper pairs that are located near the trap

edge, and that this leads to a phase separation between the nonrotating superfluid (fully paired) atoms located around the trap center and the rigidly rotating normal (nonpaired) atoms located towards the trap edge, with a coexisting (partially paired) region in between. This leads to a continuous density and superfluid order parameter as a function of radial distance. Furthermore, we show that the superfluid phase that occurs in the coexistence region is characterized by a gapless excitation spectrum, and that it is distinct from the gapped phase that occurs near the trap center.

We obtain these results by solving the mean-field BdG equations in the rotating frame (in units of $\hbar = k_B = 1$)

$$\begin{bmatrix} \mathcal{K}_\uparrow(\mathbf{r}) - \Omega \mathcal{L}_z & \Delta(\mathbf{r}) \\ \Delta^*(\mathbf{r}) & -\mathcal{K}_\downarrow(\mathbf{r}) + \Omega \mathcal{L}_z^* \end{bmatrix} \begin{bmatrix} u_\eta(\mathbf{r}) \\ v_\eta(\mathbf{r}) \end{bmatrix} = \epsilon_\eta \begin{bmatrix} u_\eta(\mathbf{r}) \\ v_\eta(\mathbf{r}) \end{bmatrix}, \quad (1)$$

where $\mathcal{K}_\sigma(\mathbf{r}) = -\nabla^2/(2M) - \mu_\sigma(r)$, Ω is the rotation frequency around the z -axis of the trapping potential, \mathcal{L}_z is the z -component of the angular momentum operator, and the off-diagonal self-consistency field $\Delta(\mathbf{r}) = g \langle \psi_\uparrow(\mathbf{r}) \psi_\downarrow(\mathbf{r}) \rangle$ is the local superfluid order parameter. Here, $\sigma \equiv \{\uparrow, \downarrow\}$ labels the trapped hyperfine states, M is the mass, $\mu_\sigma(r) = \mu_\sigma - V(r)$ is the local chemical potential, μ_σ is the global chemical potential, $V(r) = M\omega^2 r^2/2$ is the trapping potential which is assumed to be spherically symmetric, ω is the trapping frequency, $g > 0$ is the strength of the zero-ranged attractive interactions between \uparrow and \downarrow atoms, and $\langle \dots \rangle$ is a thermal average. The quasiparticle wavefunctions $u_\eta(\mathbf{r})$ and $v_\eta(\mathbf{r})$ are related to the particle annihilation operator $\psi_\sigma(\mathbf{r})$ via the Bogoliubov-Valatin transformation $\psi_\sigma(\mathbf{r}) = \sum_\eta [u_{\eta,\sigma}(\mathbf{r}) \gamma_{\eta,\sigma} - s_\sigma v_{\eta,\sigma}^*(\mathbf{r}) \gamma_{\eta,-\sigma}^\dagger]$, where $\gamma_{\eta,\sigma}^\dagger$ and $\gamma_{\eta,\sigma}$ are the quasiparticle creation and annihilation operators, respectively, and $s_\uparrow = +1$ and $s_\downarrow = -1$. Since the BdG equations are invariant under the transformation $v_{\eta,\uparrow}(\mathbf{r}) \rightarrow u_{\eta,\uparrow}^*(\mathbf{r})$, $u_{\eta,\downarrow}(\mathbf{r}) \rightarrow -v_{\eta,\downarrow}^*(\mathbf{r})$ and $\epsilon_{\eta,\downarrow} \rightarrow -\epsilon_{\eta,\uparrow}$, it is sufficient to solve only for $u_\eta(\mathbf{r}) \equiv u_{\eta,\uparrow}(\mathbf{r})$, $v_\eta(\mathbf{r}) \equiv v_{\eta,\downarrow}(\mathbf{r})$ and $\epsilon_\eta \equiv \epsilon_{\eta,\uparrow}$ as long as we keep all of the solutions with positive and negative eigenvalues.

We assume $\Delta(\mathbf{r}) = -g \sum_\eta u_\eta(\mathbf{r}) v_\eta^*(\mathbf{r}) f(\epsilon_\eta)$ is real without losing generality, where $f(x) = 1/[\exp(x/T) + 1]$ is the Fermi function and T is the temperature. Furthermore, we can relate g to the two-body scattering length a_F

via $1/g = -M/(4\pi a_F) + Mk_c(r)/(2\pi^2)$ where $k_c^2(r) = 2M[\epsilon_c + \mu(r)]$ and $\mu(r) = [\mu_\uparrow(r) + \mu_\downarrow(r)]/2$. Here, ϵ_c is the energy cutoff to be specified below, and our results depend weakly on the particular value of ϵ_c provided that it is chosen sufficiently high. The order parameter equation has to be solved self-consistently with the number equation $N_\sigma = \int d\mathbf{r} n_\sigma(\mathbf{r})$, where $n_\sigma(\mathbf{r}) = \langle \psi_\sigma^\dagger(\mathbf{r}) \psi_\sigma(\mathbf{r}) \rangle$ is the local density of fermions, leading to $n_\uparrow(\mathbf{r}) = \sum_\eta |u_\eta(\mathbf{r})|^2 f(\epsilon_\eta)$ and $n_\downarrow(\mathbf{r}) = \sum_\eta |v_\eta(\mathbf{r})|^2 f(-\epsilon_\eta)$.

Next, we expand $u_\eta(\mathbf{r})$ and $v_\eta(\mathbf{r})$ in the complete basis of the harmonic trapping potential eigenfunctions given by $\mathcal{K}_\sigma(\mathbf{r})\phi_{n,\ell,m}(\mathbf{r}) = \xi_{n,\ell}^\sigma \phi_{n,\ell,m}(\mathbf{r})$, where $\xi_{n,\ell}^\sigma = \omega(2n + \ell + 3/2) - \mu_\sigma$ is the eigenvalue and $\phi_{n,\ell,m}(\mathbf{r}) = R_{n,\ell}(r)Y_{\ell,m}(\theta_r, \varphi_r)$ is the eigenfunction. Here, n is the radial quantum number, and ℓ and m are the orbital angular momentum and its projection, respectively. The angular part $Y_{\ell,m}(\theta_r, \varphi_r)$ is a spherical harmonic and the radial part is $R_{n,\ell}(r) = \sqrt{2}(M\omega)^{3/4} [n!/(n + \ell + 1/2)!]^{1/2} e^{-\bar{r}^2/2} \bar{r}^\ell L_n^{\ell+1/2}(\bar{r}^2)$, where $\bar{r} = \sqrt{M\omega}r$ is dimensionless and $L_i^j(x)$ is an associated Laguerre polynomial.

We choose $\mathcal{L}_z = -i\partial/\partial\varphi_r$ and $\eta \equiv \{\ell, m, \gamma\}$, leading to $u_{\ell,m,\gamma}(\mathbf{r}) = \sum_n c_{\ell,m,\gamma,n} \phi_{n,\ell,m}(\mathbf{r})$ and $v_{\ell,m,\gamma}(\mathbf{r}) = \sum_n d_{\ell,m,\gamma,n} \phi_{n,\ell,m}(\mathbf{r})$. This expansion reduces the BdG equations to a $2(n_\ell + 1) \times 2(n_\ell + 1)$ matrix eigenvalue problem for a given $\{\ell, m\}$ state

$$\sum_{n'} \begin{pmatrix} K_{\uparrow,\ell}^{n,n'} - m\Omega\delta_{n,n'} & \Delta_\ell^{n,n'} \\ \Delta_\ell^{n',n} & -K_{\downarrow,\ell}^{n,n'} - m\Omega\delta_{n,n'} \end{pmatrix} \begin{pmatrix} c_{\ell,m,\gamma,n'} \\ d_{\ell,m,\gamma,n'} \end{pmatrix} = \epsilon_{\ell,m,\gamma} \begin{pmatrix} c_{\ell,m,\gamma,n} \\ d_{\ell,m,\gamma,n} \end{pmatrix}. \quad (2)$$

Here, $n_\ell = (n_c - \ell)/2$ is the maximal radial quantum number and n_c is the radial quantum number cutoff, such that we include only the single particle states with $\omega(2n + \ell + 3/2) \leq \epsilon_c = \omega(n_c + 3/2)$. In Eq. 2, the diagonal matrix element is $K_{\sigma,\ell}^{n,n'} = \xi_{n,\ell}^\sigma \delta_{n,n'}$ where $\delta_{i,j}$ is the Kronecker delta, and the off-diagonal matrix element is $\Delta_\ell^{n,n'} \approx \int r^2 dr \Delta(r) R_{n,\ell}(r) R_{n',\ell}(r)$. Although $\Delta(\mathbf{r})$ becomes axially symmetric when $\Omega \neq 0$, it is convenient to define $\Delta(r) = \int d\Omega_r \Delta(\mathbf{r})/(4\pi)$ leading to

$$\Delta(r) = -\frac{g}{4\pi} \sum_{\ell,m,\gamma,n,n'} \tilde{R}_{\ell,m,\gamma,n}^\uparrow(r) \tilde{R}_{\ell,m,\gamma,n'}^\downarrow(r) f(\epsilon_{\ell,m,\gamma}), \quad (3)$$

where we introduced $\tilde{R}_{\ell,m,\gamma,n}^\uparrow(r) = c_{\ell,m,\gamma,n} R_{n,\ell}(r)$ and $\tilde{R}_{\ell,m,\gamma,n}^\downarrow(r) = d_{\ell,m,\gamma,n} R_{n,\ell}(r)$. Similarly, we define $n_\sigma(r) = \int d\Omega_r n_\sigma(\mathbf{r})/(4\pi)$ leading to

$$n_\sigma(r) = \frac{1}{4\pi} \sum_{\ell,m,\gamma,n,n'} \tilde{R}_{\ell,m,\gamma,n}^\sigma(r) \tilde{R}_{\ell,m,\gamma,n'}^\sigma(r) f(s_\sigma \epsilon_{\ell,m,\gamma}). \quad (4)$$

Lastly, N_σ reduces to $N_\uparrow = \sum_{\ell,m,\gamma,n} c_{\ell,m,\gamma,n}^2 f(\epsilon_{\ell,m,\gamma})$ and $N_\downarrow = \sum_{\ell,m,\gamma,n} d_{\ell,m,\gamma,n}^2 f(-\epsilon_{\ell,m,\gamma})$. When $\Omega \rightarrow 0$, the eigenfunction coefficients $c_{\ell,m,\gamma,n}$ and $d_{\ell,m,\gamma,n}$ and the eigenvalues $\epsilon_{\ell,m,\gamma}$ become independent of m , and Eqs. (2), (3)

and (4) reduce to the usual ones, see *e.g.* Ref. [11, 12, 13, 14]. Therefore, due to the coupling between different m states, the rotating case is numerically much more involved compared to the nonrotating case.

In addition to $n_\sigma(r)$, we want to calculate the local density of normal (rotating) fermions $n_{\sigma,N}(r)$. For this purpose, we use the local current density $\mathbf{J}_\sigma(\mathbf{r}) = \langle \mathcal{J}_\sigma(\mathbf{r}) \rangle$, where $\mathcal{J}_\sigma(\mathbf{r}) = [1/(2Mi)][\psi_\sigma^\dagger(\mathbf{r})\nabla\psi_\sigma(\mathbf{r}) - H.c.]$ is the quantum mechanical probability current operator and $H.c.$ is the Hermitian conjugate. This leads to $\mathbf{J}_\uparrow(\mathbf{r}) = [1/(2Mi)] \sum_\eta [u_\eta^*(\mathbf{r})\nabla u_\eta(\mathbf{r})f(\epsilon_\eta) - H.c.]$ and $\mathbf{J}_\downarrow(\mathbf{r}) = [1/(2Mi)] \sum_\eta [v_\eta(\mathbf{r})\nabla v_\eta^*(\mathbf{r})f(-\epsilon_\eta) - H.c.]$. The current, similar to the classical case, can be written as $\mathbf{J}_\sigma(\mathbf{r}) = n_{\sigma,N}(\mathbf{r})\mathbf{v}(\mathbf{r})$, where $n_{\sigma,N}(\mathbf{r})$ is the local density and $\mathbf{v}(\mathbf{r}) = \Omega \hat{\mathbf{z}} \times \mathbf{r}$ is the local velocity of normal fermions corresponding to a rigid-body rotation. Since the normal fermions are expelled towards the trap edge, we approximate $n_{\sigma,N}(r) = \int d\Omega_r n_{\sigma,N}(\mathbf{r})/(4\pi)$ as

$$n_{\sigma,N}(r) \approx \frac{s_\sigma}{4\pi M\Omega r^2} \sum_{\ell,m,\gamma,n,n'} m \tilde{R}_{\ell,m,\gamma,n}^\sigma(r) \tilde{R}_{\ell,m,\gamma,n'}^\sigma(r) f(s_\sigma \epsilon_{\ell,m,\gamma}), \quad (5)$$

such that $J_\sigma(r) = \int d\Omega_r J_\sigma(\mathbf{r})/(4\pi) \sim \Omega r n_{\sigma,N}(r)$.

Having discussed the BdG formalism, next, we analyze the ground state ($T = 0$) phases for both population balanced ($N_\uparrow = N_\downarrow$ or $\mu_\uparrow = \mu_\downarrow$) and imbalanced ($N_\uparrow \neq N_\downarrow$ or $\mu_\uparrow \neq \mu_\downarrow$) Fermi gases. This is achieved by solving the BdG equations (2), (3) and (4) self-consistently as a function of the dimensionless parameter $1/(k_F a_F)$ where k_F is the Fermi momentum defined via the Fermi energy

$$\epsilon_F = \omega(n_F + 3/2) = \frac{k_F^2}{2M} = \frac{1}{2} M \omega^2 r_F^2 \approx \omega(3N)^{1/3} \quad (6)$$

and $N = N_\uparrow + N_\downarrow = (n_F + 1)(n_F + 2)(n_F + 3)/3$. Here, n_F and r_F are the corresponding Fermi level and Thomas-Fermi radius, respectively. In our numerical calculations, we choose $n_F = 15$ and $n_c = 65$, which corresponds to a total of $N = 1632$ fermions and $\epsilon_c \approx 4\epsilon_F$, respectively. Here, it is important to emphasize that we do not expect any qualitative change in our results with higher values of n_F and/or n_c , except for minor quantitative variations.

In Fig. 1, we consider a weakly interacting Fermi gas on the BCS side with $1/(k_F a_F) = -0.5$, and show $n_\sigma(r)$ and $\Delta(r)$ for nonrotating ($\Omega = 0$) and rotating ($\Omega = 0.5\omega$) cases. When $N_\uparrow = N_\downarrow$, we find that $\Delta(r)$ depletes everywhere inside the trap and especially around the trap edge. This is because it is easier to break the Cooper pairs that are located towards the trap edge in comparison to the ones that occupy the center (see below). Our result is quantitatively different from the LDA one where $\Delta(r)$ depletes only around the trap edge [10]. When $N_\uparrow = 3N_\downarrow$, in addition to such an effect, the spatial modulation of $\Delta(r)$ disappears in the rotating case as shown in Fig. 1(b). The depletion of $\Delta(r)$ leads to a decrease (increase) in $n_\sigma(r)$ around the trap center (edge) due to the centrifugal force caused by the rotation. It also leads to a phase separation between the nonrotating fully paired superfluid (FPS) atoms located around the trap center and the

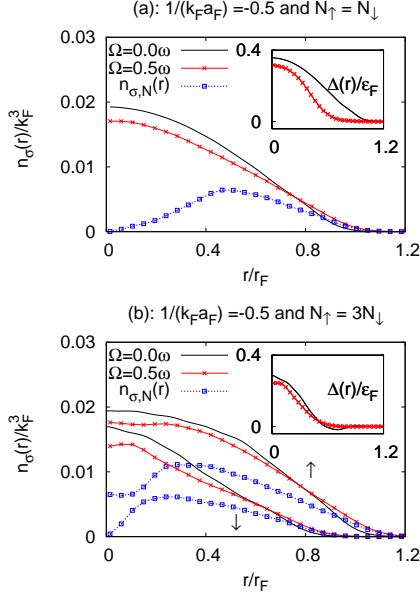


FIG. 1: We compare the density $n_\sigma(r)$ and the superfluid order parameter $\Delta(r)$ for nonrotating ($\Omega = 0$) and rotating ($\Omega = 0.5\omega$) Fermi gases. Here, $1/(k_F a_F) = -0.5$, and $N_\uparrow = N_\downarrow$ in (a) and $N_\uparrow = 3N_\downarrow$ in (b). We also show the density $n_{\sigma,N}(r)$ of normal fermions (squared-dotted line) for the rotating case.

rigidly rotating normal (nonpaired) ones located towards the trap edge, with a coexistence region in between, which is in agreement with the LDA result [10]. We characterize the FPS, coexistence and normal phases by $n_\sigma(r) \gg n_{\sigma,N}(r) = 0$, $n_\sigma(r) \gtrsim n_{\sigma,N}(r) \neq 0$ and $n_\sigma(r) = n_{\sigma,N}(r) \neq 0$, respectively. Notice that $\Delta(r)$ decreases smoothly as a function of r from the FPS to the normal region where it vanishes, which is in contrast with the LDA result where $\Delta(r)$ is nonanalytic at the transition [10]. Since $\Delta(r)$ is finite in the coexistence region, this region corresponds to a partially paired superfluid (PPS), and it occupies a larger region compared to the LDA results [10]. In addition, the trap center becomes a PPS for $\Omega \gtrsim 0.5\omega$ when $1/(k_F a_F) = -0.5$.

In Fig. 2, we consider a strongly interacting Fermi gas at unitarity with $1/(k_F a_F) = 0$, and show $n_\sigma(r)$ and $\Delta(r)$ for nonrotating ($\Omega = 0$) and rotating ($\Omega = 0.7\omega$) cases. The main effects of rotation are qualitatively similar to the weakly interacting case. However, since the Cooper pairs become more strongly bound as a function of the interaction strength, it requires much faster Ω to break them. For instance, at unitarity, the entire superfluid is robust for $\Omega \lesssim 0.3\omega$, and the trap center stays as an FPS even for $\Omega \sim \omega$ (not shown). Therefore, the effects of rotation become weaker as the interaction strength increases, and both the PPS and the normal regions eventually disappear in the molecular limit (not shown), *i.e.* rotation can not break any Cooper pair in the molecular limit.

Another important observable is the local angular momentum defined by $L_{z,\sigma}(\mathbf{r}) = \langle \psi_\sigma^\dagger(\mathbf{r}) \mathcal{L}_z \psi_\sigma(\mathbf{r}) \rangle$. This leads to $L_{z,\uparrow}(\mathbf{r}) = -i \sum_\eta v_\eta^*(\mathbf{r}) \partial u_\eta(\mathbf{r}) / \partial \varphi_\mathbf{r} f(\epsilon_\eta)$ and $L_{z,\downarrow}(\mathbf{r}) = -i \sum_\eta v_\eta(\mathbf{r}) \partial v_\eta^*(\mathbf{r}) / \partial \varphi_\mathbf{r} f(-\epsilon_\eta)$. Since the superfluid atoms

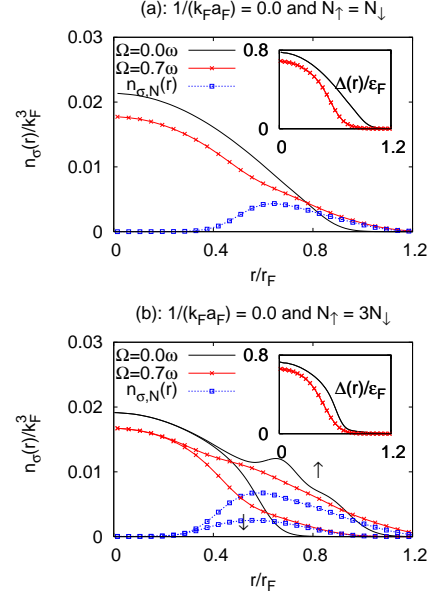


FIG. 2: We compare the density $n_\sigma(r)$ and the superfluid order parameter $\Delta(r)$ for nonrotating ($\Omega = 0$) and rotating ($\Omega = 0.7\omega$) Fermi gases. Here, $1/(k_F a_F) = 0.0$, and $N_\uparrow = N_\downarrow$ in (a) and $N_\uparrow = 3N_\downarrow$ in (b). We also show the density $n_{\sigma,N}(r)$ of normal fermions (squared-dotted line) for the rotating case.

do not carry angular momentum, $L_{z,\sigma}(\mathbf{r})$ is directly related to the local density of normal fermions via $L_{z,\sigma}(\mathbf{r}) = \int d\Omega \mathbf{r} L_{z,\sigma}(\mathbf{r}) / (4\pi) \approx M \Omega r^2 n_{\sigma,N}(r)$. Therefore, $L_{z,\sigma}(\mathbf{r})$ can be easily extracted from Figs. 1 and 2. For completeness, the total angular momentum $L_{z,\sigma} = \int d\mathbf{r} L_{z,\sigma}(\mathbf{r})$ becomes $L_{z,\uparrow} = \sum_{\ell,m,\gamma,n,n'} m c_{\ell,m,\gamma,n}^2 f(\epsilon_{\ell,m,\gamma})$ and $L_{z,\downarrow} = -\sum_{\ell,m,\gamma,n,n'} m d_{\ell,m,\gamma,n}^2 f(-\epsilon_{\ell,m,\gamma})$, and it increases with increasing Ω . In the weakly attracting limit, $L_{z,\sigma}$ becomes its rigid-body value when Ω increases high enough so that $\Delta(r) \rightarrow 0$ everywhere (not shown).

The microscopic mechanism responsible for the pair breaking effects can be understood analytically within the semiclassical LDA, *i.e.* each component of the Fermi gas is considered as locally homogenous at each position \mathbf{r} with a local chemical potential $\mu_\sigma(\mathbf{r})$. In this approximation, the local quasiparticle and quasihole excitation branches are [10, 15]

$$E_{1,2}(\mathbf{p}, \mathbf{r}) = \frac{\mu_\uparrow - \mu_\downarrow}{2} + \mathbf{v}(\mathbf{r}) \cdot \mathbf{p} \pm E_0(p, \mathbf{r}), \quad (7)$$

where $E_0(p, \mathbf{r}) = \sqrt{[p^2/(2M) - \mu(r)]^2 + \Delta^2(\mathbf{r})}$ is the usual spectrum for nonrotating and population balanced mixtures, $\mathbf{v}(\mathbf{r}) = \Omega \hat{\mathbf{z}} \times \mathbf{r}$ is the velocity and \mathbf{p} is the momentum. In Fig. 3, we present three schematic diagrams showing $E_1(\mathbf{p}, \mathbf{r})$ and $E_2(\mathbf{p}, \mathbf{r})$ as a function of \mathbf{p} for fixed values of \mathbf{r} . At each \mathbf{r} , the many-body ground state wavefunction fills up all of the states with negative energy, and excitations correspond to removing a quasiparticle or a quasihole from a filled state and adding it to the one that is not filled. In order to show that these excitation spectra correspond to three topologically distinct superfluid phases that can be observed in atomic sys-

tems, next we discuss $E_{1,2}(\mathbf{p}, \mathbf{r})$ in the $z = 0$ plane such that $\mathbf{r} \equiv (x, y, 0)$.

First, we consider the population balanced case where $\mu_\uparrow = \mu_\downarrow$. In the FPS phase, the excitation spectrum is symmetric around the zero energy axis, *i.e.* $E_1(\mathbf{p}, \mathbf{r}) = -E_2(\mathbf{p}, \mathbf{r})$, leading to a gapped spectrum as shown in Fig. 3(a). However, in the rotating case, there is a local asymmetry between the pairing states $\{\mathbf{r}, \mathbf{p}, \uparrow; \mathbf{r}, -\mathbf{p}, \downarrow\}$ and $\{\mathbf{r}, -\mathbf{p}, \uparrow; \mathbf{r}, \mathbf{p}, \downarrow\}$. When this asymmetry becomes sufficiently large, there exists a momentum space region $p_- \leq p \leq p_+$ where $E_1(-\mathbf{p}, \mathbf{r}) \leq 0$ and $E_2(\mathbf{p}, \mathbf{r}) \geq 0$. This occurs for position space region $r \geq r_T$ when the condition $A(r) = 2M\Omega^2 r^2[\mu(r) + M\Omega^2 r^2/2] - \Delta^2(r) \geq 0$ is satisfied, where r_T is defined through $A(r_T) = 0$ and $p_\pm = 2M[\mu(r) + M\Omega^2 r^2] \pm 2M\sqrt{A(r)}$. Therefore, both $E_{1,2}(\mathbf{p}, \mathbf{r})$ have two zeros at $p = p_\pm$, and the excitation spectrum becomes gapless at these momenta. We characterize this phase as the PPS, and its excitation spectrum is shown in Fig. 3(b).

For a weakly attracting gas, the condition $A(r) \geq 0$ can only be satisfied near the trap edge when $\Omega \ll \omega$, but it can also be satisfied near the trap center when $\Omega \sim \omega$. However, in the strongly interacting limit where μ is small yet positive, this condition can only be satisfied for sufficiently small values of $\Delta(r)$ near the trap edge even when $\Omega \sim \omega$. Finally, in the molecular limit where μ is negative, this condition can not be satisfied anywhere inside the trap, leading to a superfluid phase with a gapped excitation spectrum, *i.e.* the Cooper pairs are robust in the molecular limit. As one may expect, the asymmetric pairing caused by the rotation does not lead to a local population imbalance at any position r since $E_1(-\mathbf{p}, \mathbf{r}) \leq 0$ when $E_2(\mathbf{p}, \mathbf{r}) \geq 0$ and vice versa. However, this asymmetry prevents the formation of Cooper pairs in the phase space region when both $E_{1,2}(\mathbf{p}, \mathbf{r}) \geq 0$ or both $E_{1,2}(\mathbf{p}, \mathbf{r}) \leq 0$, and thus it is responsible for the creation of the PPS and the normal phases.

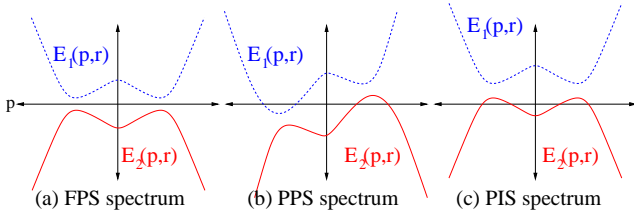


FIG. 3: Schematic diagrams showing the excitation spectrum of (a) a gapped fully paired superfluid (FPS) phase at $r = 0$, (b) a gapless partially paired superfluid (PPS) phase at $r \geq r_T$, and (c) a gapless population imbalanced superfluid (PIS) phase at $r = 0$ as a function of momentum \mathbf{p} .

We find that the local excitation spectrum changes from gapped (FPS) to gapless (PPS) at position $r = r_T$. In homogeneous (infinite) systems such a change is classified as a topological quantum phase transition [16]. Since this change occurs in the momentum space, it does not leave any strong signature in the momentum averaged observables such as $\Delta(r)$, $n(r)$, etc. However, its direct consequences can be observed via a recently developed position and momentum resolved spectroscopy [17]. For instance, the local density distributions [15]

$$n_{\uparrow, \downarrow}(\mathbf{p}, \mathbf{r}) = \tilde{u}^2(\mathbf{p}, \mathbf{r})f[\pm E_{1,2}(\mathbf{p}, \mathbf{r})] + \tilde{v}^2(\mathbf{p}, \mathbf{r})f[\pm E_{2,1}(\mathbf{p}, \mathbf{r})],$$

are nonanalytic at $p = p_\pm$ when $r \geq r_T$. Here, $\tilde{u}^2(\mathbf{p}, \mathbf{r}) = \{1 + [\epsilon(p) - \mu(r)]/E_0(\mathbf{p}, \mathbf{r})\}/2$ and $\tilde{v}^2(\mathbf{p}, \mathbf{r}) = \{1 - [\epsilon(p) - \mu(r)]/E_0(\mathbf{p}, \mathbf{r})\}/2$ are the usual coherence factors with $\epsilon(p) = p^2/(2M)$.

For population imbalanced superfluids (PIS) where $\mu_\uparrow \neq \mu_\downarrow$, the excitation branches shift upwards (downwards), and one of them cross zero energy axis when $N_\uparrow > N_\downarrow$ ($N_\uparrow < N_\downarrow$), leading to a gapless excitation spectrum. This is expected since the excess fermions can only exist in regions with both $E_{1,2}(\mathbf{p}, \mathbf{r}) \geq 0$ or both $E_{1,2}(\mathbf{p}, \mathbf{r}) \leq 0$. In the absence of rotation [15], for a weakly attracting PIS only one of the excitation branches has four zeros as shown in Fig. 3(c) for the $N_\uparrow > N_\downarrow$ case. However, in the strongly attracting limit, this branch has only two zeros (not shown). When the system is rotating, the excitation spectra tilt similar to that shown in Fig. 3(b) (not shown). We remark in passing that a similar quantum phase transition with its experimental signatures has recently been discussed in the context of trapped p -wave superfluids [18].

To conclude, we used the BdG formalism to analyze the effects of adiabatic rotation on the ground state phases of harmonically trapped Fermi gases. We found that the rotation breaks Cooper pairs that are located near the trap edge, and that this leads to a phase separation between the nonrotating superfluid (fully paired) atoms located around the trap center and the rigidly rotating normal (nonpaired) atoms located towards the trap edge with a coexistence (partially paired) region in between. We also showed that the rotation reveals a topological quantum phase transition in the momentum space as a function of radial distance. An interesting extension of our work is to study emergence of dynamic instabilities for fast enough rotation [8, 19].

-
- [1] *Ultra-cold Fermi Gases*, Procs. of the Int. Sch. of Phys. ‘Enrico Fermi’, Course CLXIV, Varenna 2006, ed. by M. Inguscio, W. Ketterle, and C. Salomon (IOS Press, Amsterdam, 2008).
 - [2] S. Giorgini, L. P. Pitaevskii, and S. Stringari, *Rev. Mod. Phys.* **80**, 1215 (2008).
 - [3] N. Nygaard, G. M. Bruun, C. W. Clark, and D. L. Feder, *Phys.*

- Rev. Lett.* **90**, 210402 (2003).
- [4] M. Machida and T. Koyama, *Phys. Rev. Lett.* **94**, 140401 (2005).
- [5] R. Sensarma, M. Randeria, and Tin-Lun Ho, *Phys. Rev. Lett.* **96**, 090403 (2006).
- [6] M. W. Zwierlein *et al.*, *Nature (London)* **435**, 1047 (2005).

- [7] M. W. Zwierlein *et al.*, Science **311**, 492 (2006).
- [8] I. Bausmerth, A. Recati, and S. Stringari, Phys. Rev. Lett. **100**, 070401 (2008); and Phys. Rev. A **78**, 063603 (2008).
- [9] Hui Zai and Tin-Lun Ho, Phys. Rev. Lett. **97**, 180414 (2006).
- [10] Michael Urban and Peter Schuck, Phys. Rev. A **78**, 011601(R) (2008).
- [11] Y. Ohashi and A. Griffin, Phys. Rev. A **72**, 013601 (2005).
- [12] P. Castorina *et al.*, Phys. Rev. A **72**, 025601 (2005).
- [13] T. Mizushima *et al.*, J. Phys. Soc. Jpn. **76**, 104006 (2007).
- [14] L. M. Jensen, J. Kinnunen, and P. Törmä, Phys. Rev. A **76**, 033620 (2007).
- [15] M. Iskin and C. A. R. Sá de Melo, Phys. Rev. A **76**, 013601 (2007).
- [16] G. E. Volovik, cond-mat/0601372 (2006).
- [17] J. T. Stewart, J. P. Gaebler, and D. S. Jin, Nature **454**, 744 (2008).
- [18] M. Iskin and C. J. Williams, Phys. Rev. A **77**, 041607(R) (2008).
- [19] G. Tonini, F. Werner, and Y. Castin, Eur. Phys. J. D **39**, 283 (2006).